IEEE Access
Multidisciplinary ⋮ Rapid Review ⋮ Open Access Journal

Received 15 February 2023, accepted 3 March 2023, date of publication 9 March 2023, date of current version 3 April 2023.

Digital Object Identifier 10.1109/ACCESS.2023.3254901

RESEARCH ARTICLE

A Wide Range Distributed Multi-Node Receive Chain Calibration Method Based on GNSS Software Receiver

SHUANGZHI XIA, ZHAO ZHAO, XUWANG ZHANG, AND YOUYONG LIU
The 54th Research Institute of China Electronics Technology Group Corporation, Shijiazhuang 100081, China
Corresponding author: Zhao Zhao (18600623236@163.com)

ABSTRACT The phase calibration of distributed multi-node receiving system is required considering the phase synthesis working mode of distributed radar system for echo signals. Whereas, in respect to the traditional calibration tower and unmanned aerial vehicle scheme, there are many disadvantages. The wide range distributed multi-node receive chain calibration method based on GNSS software receiver was proposed in this paper, taking advantage of the software receiver to calculate and obtain the actual phase difference among the receiving nodes as well as the coordinate information of satellites in transmitting signal. Therefore, the phase difference resulted from different transmit path can be deleted, and the phase inconsistencies among the receiving nodes can be obtained. Besides, the fingerprint maps database regarding inconsistencies among nodes and two-dimensional angle of relative receiving node for satellites was constructed in this paper, the correspondence between the omnidirectional two-dimensional angle and the inconsistencies among different nodes was established by the actual results and two-dimensional fitting, and the phase inconsistency results among nodes can be obtained only by solving the satellite coordinate information. There are many advantages for the method proposed in this paper, such as slight influence of multipath effect, capability of all-weather all-day calibration, low costs.

INDEX TERMS GNSS, distributed multi-node receiving system, phase calibration.

I. INTRODUCTION

It is required to realize the phase synthesis of the received, especially the phase alignment of the radio frequency carrier required for the transmission coherence in the receiving working mode of the distributed radar system, which puts forward high phase accuracy requirements for the time-frequency source, baseband equipment, antenna reference point and phase center of the system. Hence, the calibration for receive chain is necessary.

Currently, the common methods for calibrating the receive chain of distributed radar nodes include two types: the tower scheme and the unmanned aerial vehicle scheme:

1. The principle of the calibration tower scheme is: the beacon machine is placed on the top of the standard calibration tower, and the nodes receive the calibration signal transmitted by the beacon machine to obtain the actual phase difference of the receive chain among the nodes (shown in Figure 1). With the assistance of the electronic distance measuring (EDM) device, the local coordinate system is established. The coordinates of the beacon machine and the receiving node are obtained under the same coordinate system. The phase difference of the calibration signal caused by transmission path between the beacon machine and different nodes can be calculated. After removing phase difference caused by transmission path, the phase inconsistency of the receive chain among nodes can be obtained [1], [2], [3], [4].

The scheme is relatively mature. The relative position of the calibration tower and the receiving nodes is fixed, and the historical record data can be used repeatedly. The receiving nodes calibration cost is low and conveniently to realize. However, there are two problems limited by the height of the calibration tower: 1) the height of the calibration tower is low to the node distribution area causing the distant nodes may be occluded. The working range cannot cover the nodes distributed in a large area; 2) the low elevation angle of

The associate editor coordinating the review of this manuscript and approving it for publication was Poki Chen.

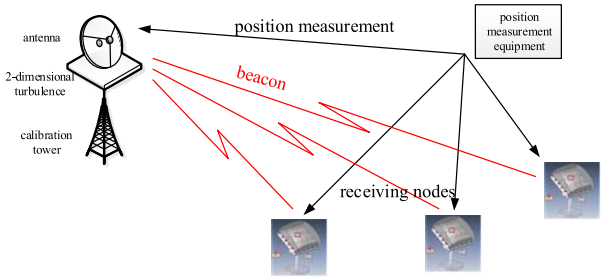

FIGURE 1. Receive chain calibration scheme based on calibration tower.

the relative node of the calibration tower leads to a strong multipath effect seriously affects the calibration accuracy.

2. The principle of the unmanned aerial vehicle scheme is: the unmanned aerial vehicle placed beacon machine flies to the predetermined airspace hover (shown in Figure 2). The range between the unmanned aerial vehicle and the node antenna phase center is measured. The phase change of the calibration signal caused by the path between the beacon machine and the receiving node can be calculated. The nodes receive the beacon signal, obtain the actual phase difference of the receive chain among the nodes, and remove the phase difference caused by the different transmission path to calculate the phase inconsistency of the receive chain [5], [6].

The unmanned aerial vehicle's solution can improve the influence of low elevation angle multipath effect on calibration results in calibration tower scheme. In addition, the path of the drone can be planned so that the nodes receive the calibration signal in all directions, thereby eliminating the phase difference caused by the different directions of the signal incident antenna. However, the problem with the unmanned aerial vehicle calibration scheme is that due to the long baseline of the distributed node (much larger than the carrier wavelength), the coordinate measurement error of the antenna phase center of the unmanned aerial vehicle is very sensitive to the influence of the results. Although the high-precision real-time kinematic (RTK) equipped with the unmanned aerial vehicle can significantly improve the accuracy of the unmanned aerial vehicle's phase center measurement, it still cannot overcome the coordinate drift problem of the unmanned aerial vehicle under the influence of high air current. In addition, the unmanned aerial vehicle calibration scheme requires the cooperation of professional pilots, and is greatly affected by the weather, which cannot meet the low-cost all-weather all-day calibration requirements.

Global navigation satellite system (GNSS) is a satellite-referenced radio navigation system. Reference datums are moving medium-orbit satellites and synchronous satellites, whose orbits are known. At present, the existing satellite navigation and positioning systems in the world mainly include the GPS system of the United States, the GLONASS system of Russia, the Beidou system of China and the Galileo system of the European Union, providing users with large-range, high-precision and fast positioning services.

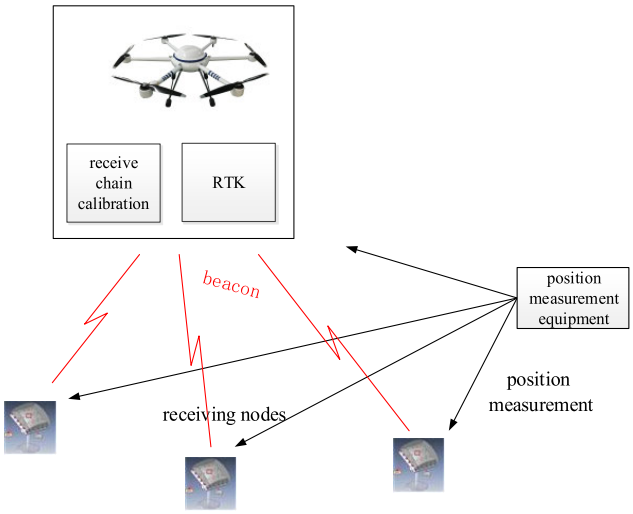

FIGURE 2. Unmanned aerial vehicle based receive chain calibration scheme.

The GNSS system broadcasts navigation message modulated on the L2C (frequency 1227.6MHz, GPS as an example) carrier, including satellite ephemeris, satellite clock error correction parameters, ranging time markers and other information, to users on the ground.

If the working frequency band of the distributed multi-node receiving system covers the L2C carrier, the software receiver can be used to acquire and track GNSS signal, demodulate navigation messages and other steps to extract the time-varying WGS-84 coordinates of the satellite, so as to use the GNSS satellite as a "beacon machine" to complete the calibration of the receive chain.

The application of GNSS signal-based receive chain calibration scheme has the following benefits: 1) Due to the long distance (10,000 kilometers) of GNSS satellites to receiving nodes, the measurement error of satellite and node coordinates has little impact on the calibration results. In addition, the satellite has a high elevation angle relative to the receiving node, and the multipath effect has little effect; 2) The GNSS signal transmitted by multiple satellites can simultaneously calibrate the same receive chain in different directions to compound results; 3) Since the relative position of satellites and receive nodes will change over time, the scheme can be calibrated with the receive chain in different directions; 4) GNSS satellite signals are not affected by the weather, which can meet the requirements of all-weather all-day calibration; 5) The calibration scheme costs very low because it does not need to add any hardware but carry out the program development of the software receiver and subsequent phase difference calculation.

II. WIDE RANGE DISTRIBUTED MULTI-NODE RECEIVE CHAIN CALIBRATION METHOD BASED ON GNSS SOFTWARE RECEIVER

The basic components of the radar system are antenna, data transmission line and processing centers which is shown

in Figure 3. The antenna is used for receiving the RF signal transmitted by radio source and transform the RF signal into IF signal. The IF signal is transmitted by the data transmission line (which called receive chain) to data processing center. The processing center processes IF signal and obtains the information of radio source.

In order to improve the SNR without significantly increasing the cost, distributed radar technology is proposed and applied. The distributed receiving nodes receive the RF signal separately. Different IF signals are transmitted to data processing center with different phase.

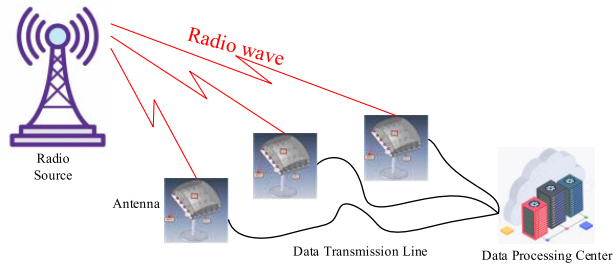

FIGURE 3. Signal two-dimensional search method.

The radar capabilities is affect by signal power synthesis efficiency which is reflected with phase difference of IF signals. According to previous project experience, in order to improve the signal detection efficiency, signal power synthesis efficiency cannot be lower than 80%. According to the simulation (shown in Figure 4), in order to achieve the requirement of signal power synthesis efficiency, the standard deviation of signal phase difference with different number of receive nodes cannot be higher than about 30°.

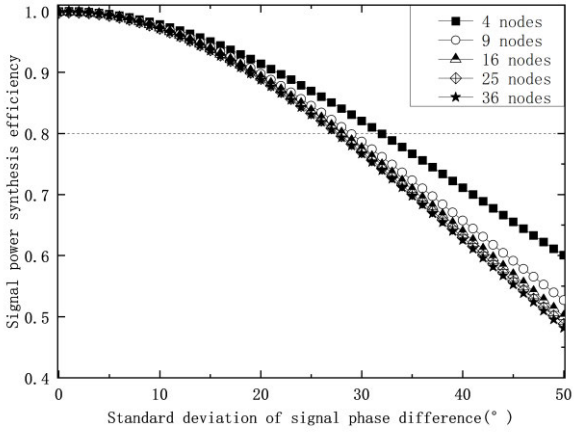

FIGURE 4. Standard deviation of signal phase difference with different number of receive nodes.

In the proposed method, before receiving the interested signal, the receive chain calibration based on GNSS of the receiving nodes should be implemented.

After receiving GNSS signal by the system, the software receiver converts signal into IF signals and processes acquisition, tracking and demodulation. The baseband signal processing is realized by software, only need to change the program settings to process other frequency bands, modulation methods and coding methods. By adjusting the parameters to make the acquisition and tracking performance the best, it has great flexibility.

The generated local signal is aligned with the carrier phase of the received GNSS signal after signal tracking. The actual phase difference among receive chains can be calculated. The actual phase difference includes the phase difference resulted from different transmission path and the phase inconsistencies between receive chains. After removing the phase difference resulted from different transmission path, it is considered that the phase inconsistencies of the receive chain is obtained.

Furthermore, the fingerprint maps database regarding inconsistencies among nodes and two-dimensional angle of relative receiving node for satellites was constructed in this paper. The correspondence between the omnidirectional two-dimensional angle and the inconsistencies among different nodes was established by the actual result. The phase inconsistency can be obtained only by solving the satellite coordinate.

A. GNSS SIGNAL PROCESSING

The navigation message broadcast by the GNSS signal contains satellite ephemeris, satellite clock error correction parameters, ranging time mark, atmospheric refraction correction parameters and other information, providing a data basis for GNSS system navigation and positioning [7], [9].

The purpose of GNSS signal acquisition is to identify all satellites within the visibility range of the receiving nodes. Due to the Doppler effect caused by the relative motion of the satellite and the nodes, the actual carrier frequency of the GNSS signal is different from nominal value. When acquiring a satellite, the signals of non-target satellites can be suppressed according to the correlation of different satellite pseudo-codes. The received signal is mixed with the local signal to filter out the carrier of the received signal. It is necessary to ensure that the frequency of the locally generated signal is close to the frequency of the received signal. In addition, in order to avoid losing useful signal components, the initial phase of the locally generated pseudo-code must be aligned with the beginning of the pseudo-code of the received signal.

GNSS signal acquisition can obtain a rough estimate of carrier frequency and code phase, and provide the tracking range for subsequent signal tracking, which is the first step in GNSS navigation solution. For stationary nodes, the Doppler frequency shift caused by relative motion does not exceed 5kHz. Based on the intermediate frequency, set the search step size and the search range of 5kHz. The code phase search step size can be set according to the acquisition accuracy requirements. The basic principle of two-dimensional search of GNSS signal is shown in Figure 5.

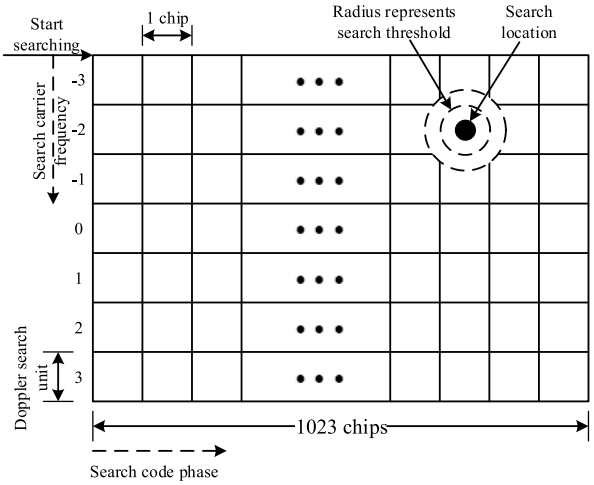

FIGURE 5. Signal two-dimensional search method.

It is necessary to design a frequency and code phase tracking loop to track changes in Doppler frequency shift and code phase, and realize synchronization between the locally generated signal and the carrier phase and pseudo-code in the GNSS signal, so as to continuously demodulate the navigation information.

The tracking loop includes a code tracking loop and a carrier tracking loop, and working principle is shown in Figure 6. The local carrier generator generates a local carrier signal with a phase difference of 90° on in-phase branch and quadrature branch. Local pseudo-code generator generate early, present and lagging codes in I branch and Q branch respectively. The IF signal received by the receiver is multiplied and mixed with the carrier replication signal generated by the local carrier generator in the IQ branches through a mixer respectively. Signals I and Q is then correlated with the early, present and lagging codes and obtain I_E, I_P, I_L, Q_E, Q_P and Q_L after integral accumulation. Then, I_P and Q_P are used as the input of the carrier loop discriminator, and I_E, I_L, Q_E, and Q_L are used as the input of the code loop discriminator. Finally, the outputs of carrier loop discriminator and code loop discriminator are respectively input to carrier loop filter and code loop filter, and the filtering results are used to adjust the output phase and frequency of the respective local carrier and pseudo-code, so that the local carrier and pseudo-code are consistent with the received signal [10].

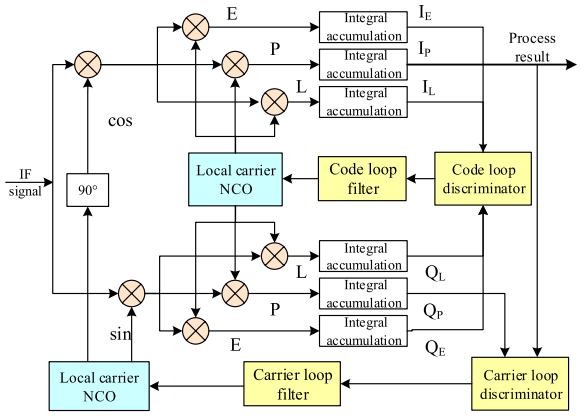

FIGURE 6. GNSS signal tracking.

After the GNSS signal tracking loop is locked, the original navigation message can be output (1000bps), and the 50Hz navigation message can be obtained after performing bit synchronization, sub-frame synchronization, and parity check on the data. Extract information such as orbital perturbation parameters, time parameters, and Kepler parameters for calculating GNSS satellite parameters are obtained by decoding the navigation message. The process is shown in Figure 7.

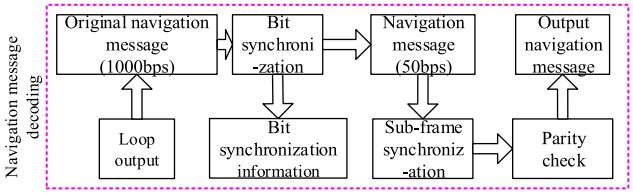

FIGURE 7. Navigation message decoding.

B. PHASE INCONSISTENCY CALCULATION OF RECEIVE CHAIN

Considering that after the receiving nodes are put into use, the antenna coordinates will be determined accordingly. In order to simplify the process without loss of generality, we consider setting the antenna in a specific state (for example, the antenna is vertically facing the sky), and obtain the WGS-84 coordinates of the phase center of the antenna in this state through a high-precision position measurement scheme. When the orientation of the antenna changes, the coordinates of the phase center of the antenna in the new state can be deduced by establishing a coordinate system with the phase center of the antenna as the local coordinate system.

The ephemeris of a satellite can be viewed as a function of the independent variable in time of the satellite's motion. The coordinates $(x_{sat}, y_{sat}, z_{sat})$ of the T moment satellite can be obtained through the CNAV decoding module of the software receiver and the satellite coordinate calculation module. The coordinate of the satellite's WGS-84 is $(x_{sat}, y_{sat}, z_{sat})$, transmitting GNSS data segment S. The data segment S is received by node A and node B (phase center coordinates are calibrated by high-precision position measurement method, (x_A, y_A, z_A), (x_B, y_B, z_B), respectively) through different path transmissions. The phase detector of the software receiver produces the actual phase difference φ_e of data segment S between two receive nodes. This carrier phase difference mainly contains two parts: one is the phase difference φ_{range} caused by the different transmission path R, and the other is the phase inconsistency of the receive chain between the two nodes $\Delta\varphi$. It can be expressed as:

$$\varphi_e = \varphi_{range} + \Delta\varphi \tag{1}$$

Combined with the coordinates of the satellite and the nodes, the phase difference φ_{range} caused by different transmission path R can be calculated as:

$$\begin{aligned}\varphi_{range} &= rem\,(R,\lambda)\big/\lambda * 2\pi \\ R &= \sqrt{(x_{sat}-x_B)^2+(y_{sat}-y_B)^2+(z_{sat}-z_B)^2} \\ &\quad -\sqrt{(x_{sat}-x_A)^2+(y_{sat}-y_A)^2+(z_{sat}-z_A)^2}\end{aligned} \tag{2}$$

Among them, rem (A, B) is the remainder of A divided by B, and λ is the wavelength of GNSS signal; (x_0, y_0, z_0) is coordinate of receiving antenna phase center. We assume that R is positive.

The receive chain phase inconsistency between two nodes can be reduced to:

$$\Delta\varphi = \varphi_e - \varphi_{range} = \varphi_e - rem\,(R,\lambda)\big/\lambda * 2\pi \tag{3}$$

The above process is shown in Figure 8:

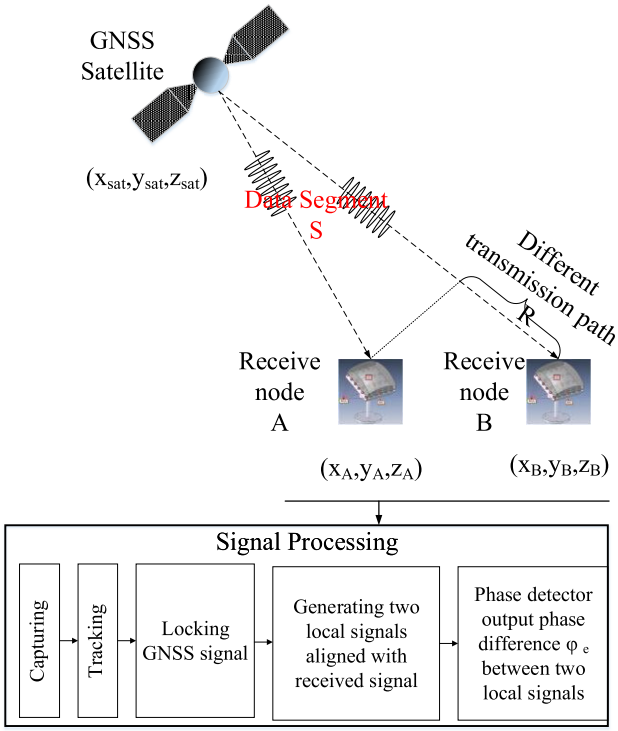

FIGURE 8. Schematic diagram of two nodes receiving GNSS signals.

C. CONSRTUCTION OF FINGERPRINT MAPS DATABASE

It is easy to know that the elevation angle θ, azimuth angle α and distance r of the satellite obtained under the local ENU coordinate system established with the antenna phase center of the receiving node as the origin uniquely correspond to the phase inconsistency $\Delta\varphi$ of the receiving chain. This paper considers adopting two-dimensional directional angle fingerprint database for the phase inconsistency between the two-dimensional direction angle-node, so that when the satellite coordinates are settled, the corresponding inter-node phase inconsistencies can be searched in the fingerprint database, and the receive chain calibration between nodes can be quickly completed.

And in the process of constructing the fingerprint database, when enough data is collected, fitting can be performed to complete the establishment of the omnidirectional fingerprint database. At this time, considering the use of two-dimensional angle fingerprint library is more accurate than the satellite WGS-84 coordinates three-dimensional fingerprint database, less measurement points are required.

The conversion process is shown as below:

$$\begin{bmatrix} e \\ n \\ u \end{bmatrix} = \begin{bmatrix} -\sin(lon_0) & \cos(lon_0) & 0 \\ -\sin(lat_0)\cos(lon_0) & -\sin(lat_0)\sin(lon_0) & \cos(lat_0) \\ \cos(lat_0)\cos(lon_0) & \cos(lat_0)\sin(lon_0) & \sin(lat_0) \end{bmatrix} \cdot \left(\begin{bmatrix} x_{sat} \\ y_{sat} \\ z_{sat} \end{bmatrix} - \begin{bmatrix} x_0 \\ y_0 \\ z_0 \end{bmatrix} \right) \tag{4}$$

$(x_{sat}, y_{sat}, z_{sat})$ is the WGS-84 coordinate of the satellite; (x_0, y_0, z_0) is the WGS-84 coordinate of the antenna phase center; lon_0, lat_0, alt_0 is the longitude, latitude and altitude of the antenna phase center, which can be obtained by high-precision measurement.

The elevation angle θ, azimuth angle α and distance r of the satellite can be calculated by the following equation:

$$\begin{aligned}\theta &= \arcsin\left(\frac{u}{\sqrt{e^2+n^2+u^2}}\right) \\ \alpha &= \arctan\left(\frac{e}{n}\right) \\ r &= u\end{aligned} \tag{5}$$

During the operation of the satellite, the WGS-84 coordinates at two moments are $(x_{sat1}, y_{sat1}, z_{sat1})$ and $(x_{sat2}, y_{sat2}, z_{sat2})$(shown in Figure 9). The elevation angle, azimuth angle and distance to the antenna phase center (x_0, y_0, z_0) are $(\theta_1, \alpha_1, r_1)$ and $(\theta_2, \alpha_2, r_2)$ respectively. The phase inconsistencies are calculated as $\Delta\varphi_1$ and $\Delta\varphi_2$. And the correspondences can be expressed as:

$$\begin{bmatrix} (\theta_1,\alpha_1) \Leftrightarrow \Delta\varphi_1 \\ (\theta_2,\alpha_2) \Leftrightarrow \Delta\varphi_2 \end{bmatrix} \tag{6}$$

After continuously collect the data of the specific satellite (which can be determined by the pseudo-code PRN number), considering the smoothness of the satellite's orbit, a complete fingerprint map can be established by two-dimensional fitting:

$$[A \Rightarrow B] = \begin{bmatrix} (\theta_1,\alpha_1) \Leftrightarrow \Delta\varphi_1 \\ (\theta_2,\alpha_2) \Leftrightarrow \Delta\varphi_2 \\ \cdots \\ (\theta_n,\alpha_n) \Leftrightarrow \Delta\varphi_n \end{bmatrix} \tag{7}$$

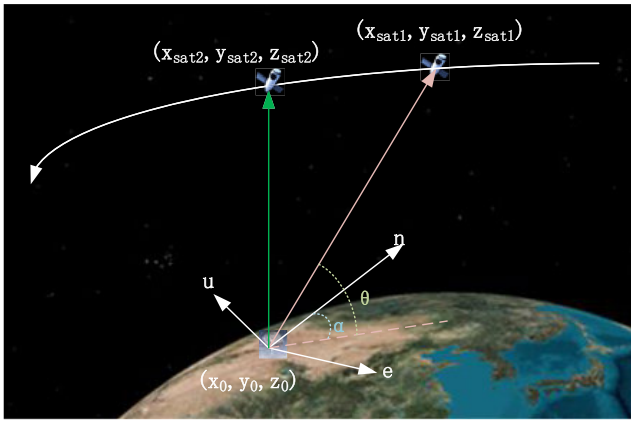

FIGURE 9. Schematic diagram of establishing a two-dimensional angle-phase inconsistency fingerprint library during satellite motion.

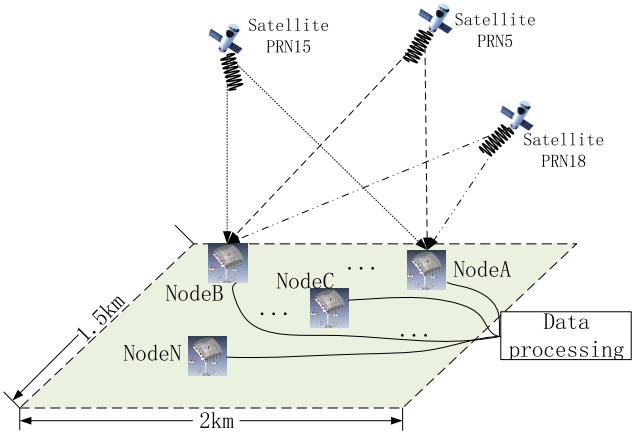

FIGURE 10. Schematic diagram of distributed node verification test system.

$[A \Rightarrow B]$ indicates that the ENU coordinate system is established with the antenna phase center of node B, and the phase inconsistency of the receiving chain between NodeA to NodeB. When there are N distributed nodes, it is necessary to establish correspondences with number of C_N^2. If we build $[A \Rightarrow B]$, the $[B \Rightarrow A]$ can be easily obtained:

$$[B \Rightarrow A] = \begin{bmatrix} (\theta_1, \alpha_1) \Leftrightarrow -\Delta\varphi_1 \\ (\theta_2, \alpha_2) \Leftrightarrow -\Delta\varphi_2 \\ \cdots \\ (\theta_n, \alpha_n) \Leftrightarrow -\Delta\varphi_n \end{bmatrix} \tag{8}$$

III. EXPERIMENT RESULT

The verification system is shown in Figure 10. There are three satellites transmit GNSS signals which PRN are 5, 15 and 18.

We built an experiment verifying system which the receiving nodes are distributed in the 2km*1.5km area. The atmospheric transmission delay can be considered unanimous under the short baseline (kilometer level) condition. The distributed nodes are marked as NodeA, NodeB…, NodeN. All the nodes are connected with data processing module which is used to process GNSS signals and calculate actual phase difference. The different receive chain of nodes to data processing model leads to phase inconsistency.

After continuously collect the data and two-dimensional fitting, a system complete fingerprint map is built up. The system complete fingerprint map is shown as follows, equation (9), as shown at the bottom of the page.

We receive satellite data for another time. After solving the coordinates of the satellite, the phase inconsistencies can be searched from the system complete fingerprint map. The phase inconsistencies between NodeB to NodeA, NodeC to NodeA, NodeC to NodeB are shown in Figure 11 and Table 1. The average phase inconsistency of NodeB to NodeA is 4.01°, 7.24° and 7.65° results from satellite PRN5, PRN15 and PRN18 respectively. So the phase inconsistency of NodeB to NodeA can be regarded as 6.3°. Similarly, the phase inconsistencies of NodeC to NodeA and NodeC to NodeB can be calculated as 15.74° and 10.91°. The standard deviation of phase inconsistency can also be calculated as 2.29°, 1.81° and 2.41°. It can be seen that, within 60s signal receiving, the phase inconsistencies of nodes is stable. The results of three satellites are so close, proving that the

$$PRN5/15/18 = \left\{ \begin{array}{lll} [B \Rightarrow A] = \begin{bmatrix} (\theta_1, \alpha_1) \Leftrightarrow \Delta\varphi_1 \\ (\theta_2, \alpha_2) \Leftrightarrow \Delta\varphi_2 \\ \cdots \\ (\theta_n, \alpha_n) \Leftrightarrow \Delta\varphi_n \end{bmatrix} & & \\ [C \Rightarrow A] = \begin{bmatrix} (\theta_1, \alpha_1) \Leftrightarrow \Delta\phi_1 \\ (\theta_2, \alpha_2) \Leftrightarrow \Delta\phi_2 \\ \cdots \\ (\theta_n, \alpha_n) \Leftrightarrow \Delta\phi_n \end{bmatrix} & [C \Rightarrow B] = \begin{bmatrix} (\theta_1, \alpha_1) \Leftrightarrow \Delta\xi_1 \\ (\theta_2, \alpha_2) \Leftrightarrow \Delta\xi_2 \\ \cdots \\ (\theta_n, \alpha_n) \Leftrightarrow \Delta\xi_n \end{bmatrix} & \cdots \\ \vdots & \vdots & \ddots \\ [N \Rightarrow A] = \begin{bmatrix} (\theta_1, \alpha_1) \Leftrightarrow \Delta\psi_1 \\ (\theta_2, \alpha_2) \Leftrightarrow \Delta\psi_2 \\ \cdots \\ (\theta_n, \alpha_n) \Leftrightarrow \Delta\psi_n \end{bmatrix} & [N \Rightarrow B] = \begin{bmatrix} (\theta_1, \alpha_1) \Leftrightarrow \Delta\zeta_1 \\ (\theta_2, \alpha_2) \Leftrightarrow \Delta\zeta_2 \\ \cdots \\ (\theta_n, \alpha_n) \Leftrightarrow \Delta\zeta_n \end{bmatrix} & \cdots \end{array} \right\} \tag{9}$$

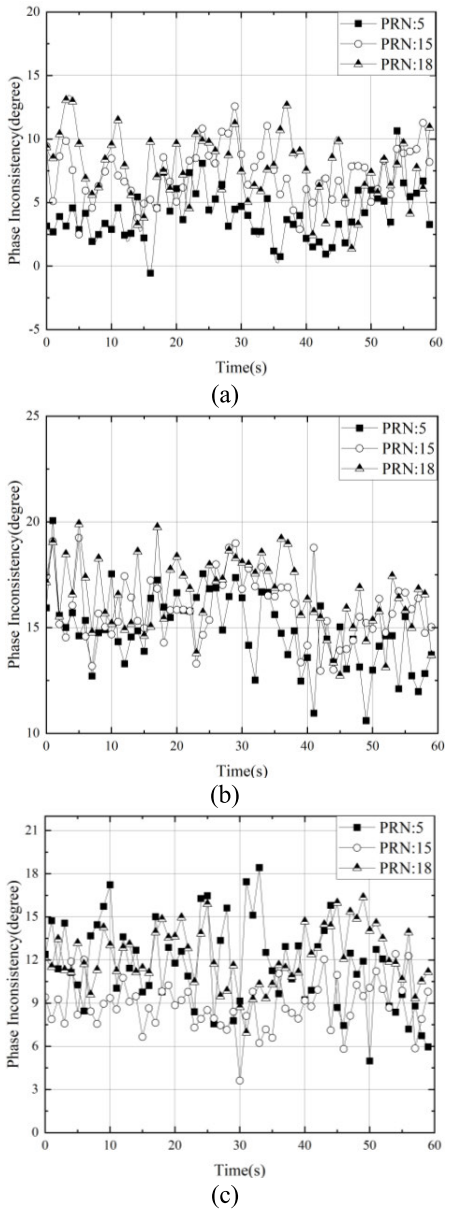

FIGURE 11. The phase inconsistency changes within 1 min. (a) NodeB to NodeA; (b) NodeC to NodeA; (c) NodeC to NodeB.

proposed method is feasible. By the same way, the phase inconsistencies of other nodes and satellites can also obtained.

Considering the antenna anisotropy, we experiment more GNSS data for calibration the same nodes as shown before.

The results of phase inconsistency of nodes (NodesA/ NodesB/ NodesC) with long-term operation are shown in TABLE 2 & TABLE 3.

It can be seen that, the standard deviation of phase inconsistency of distributed nodes can be controlled within 30°, which make the signal power synthesis efficiency higher than 80%. The calibration of multiple satellites with different direction at same time verify the advantage of the proposed method.

TABLE 1. Phase inconsistency of nodes.

Satellite PRN	NodeB to NodeA	NodeC to NodeA	NodeC to NodeB
PRN 5	*4.01*	*14.84*	*11.65*
PRN 15	*7.24*	*15.86*	*8.85*
PRN 18	*7.65*	*16.52*	*12.24*
Average phase inconsistency of 3 satellites (°)	*6.3*	*15.74*	*10.91*
Standard deviation of phase inconsistency (°)	*2.29*	*1.81*	*2.41*

TABLE 2. Phase inconsistency of nodes (afternoon).

Satellite PRN	NodeB to NodeA	NodeC to NodeA	NodeC to NodeB
PRN 5	*6.34*	*16.03*	*9.59*
PRN 15	*5.13*	*14.24*	*10.15*
PRN 18	*6.37*	*14.62*	*11.07*
Average phase inconsistency of 3 satellites (°)	*5.95*	*14.96*	*10.27*
Standard deviation of phase inconsistency (°)	*1.96*	*1.85*	*2.92*

TABLE 3. Phase inconsistency of nodes (night).

Satellite PRN	NodeB to NodeA	NodeC to NodeA	NodeC to NodeB
PRN 5	*6.12*	*14.43*	*11.31*
PRN 15	*7.8*	*14.21*	*13.07*
PRN 18	*7.35*	*15.85*	*9.21*
Average phase inconsistency of 3 satellites (°)	*7.09*	*14.83*	*11.19*
Standard deviation of phase inconsistency (°)	*2.08*	*4.24*	*2.57*

It can be also shown that, the proposed method can meet the requirements of all-day calibration.

IV. CONCLUSION

We propose a wide range distributed multi-nodes receive chain calibration method based on GNSS software receiver. The actual phase difference among receiving nodes can be calculated by software receiver, after deleting phase difference resulted from different transmitting path, the phase inconsistencies among the receiving nodes can be obtained. Besides, the fingerprint maps database regarding inconsistencies among nodes and two-dimensional angle of relative receiving node for satellites was constructed in this paper. After continuously collect actual data and two-dimensional fitting, a system complete fingerprint map is built up. The inconsistency result can be obtained only by solving the satellite coordinate information. We built up a distributed multi-nodes system to verify the proposed method. The long-term experiment results shows that, within 60s signal receiving, the phase inconsistencies of nodes is stable.

The results of three satellites are so close, proving that the proposed method is feasible. The method proposed in this paper has many advantages such as slight influence of multi-path effect, capability of all-weather all-day calibration, low costs and so on.

REFERENCES

[1] D. McWatters, A. Freedman, T. Michel, and V. Cable, "Antenna auto-calibration and metrology approach for the AFRL/JPL space based radar," in *Proc. IEEE Radar Conf.*, Apr. 2004, pp. 21–26, doi: 10.1109/NRC.2004.1316389.
[2] L. Lengier and R. Farrell, "'Amplitude and phase mismatch calibration testbed for 2×2 tower-top antenna array system," in *Proc. China-Ireland Int. Conf. Inf. Commun. Technol.*, Aug. 2007, pp. 165–172, doi: 10.1049/cp:20070696.
[3] D. Asztely, A. L. Swindlehurst, and B. Ottersten, "Auto calibration for signal separation with uniform linear arrays," in *Proc. 13th Int. Conf. Digit. Signal Process.*, Jul. 1997, pp. 403–406, doi: 10.1109/ICDSP.1997.628127.
[4] N. B. Shelton and B. D. Jeffs, "A robust iterative algorithm for wireless MIMO array auto-calibration," in *Proc. IEEE Int. Conf. Acoust., Speech, Signal Process.*, May 2004, pp. ii–341, doi: 10.1109/ICASSP.2004.1326264.
[5] M. O'Droma, "Development of a robust smart antenna array signal-processing algorithmbased on antenna array auto-calibration using GPS signals," Limerick Univ., Limerick, Ireland, Tech. Rep., 2002.
[6] H. S. Mir, "Calibration techniques for UAV antenna arrays," *J. Intell. Robotic Syst.*, vol. 61, nos. 1–4, pp. 513–525, Jan. 2011.
[7] O. Kyle, "Navigation signal processing for GNSS software receivers," *Geomatica*, vol. 65, no. 1, pp. 117–119, 2011.
[8] T. E. Humphreys, M. L. Psiaki, P. M. Kintner, and B. M. Ledvina, "GNSS receiver implementation on a DSP: Status, challenges, and prospects," in *Proc. 19th Int. Tech. Meeting Satell. Division Inst. Navigat. (ION GNSS)*, Sep. 2006, pp. 2370–2382. [Online]. Available: http://hdl.handle.net/2152/63323
[9] J.-C. Juang and Y.-H. Chen, "Phase/frequency tracking in a GNSS software receiver," *IEEE J. Sel. Topics Signal Process.*, vol. 3, no. 4, pp. 651–660, Aug. 2009.
[10] F. Prades, "Accelerating GNSS software receivers," in *Proc. 29th Int. Tech. Meeting Satell. Division Inst. Navigat. (ION GNSS+)*, Sep. 2016, pp. 44–61, doi: 10.33012/2016.14576.

SHUANGZHI XIA was born in Hubei, China. He received the Ph.D. degree from Xidian University. He is currently with the CETC Network Communication Research Institute.

ZHAO ZHAO was born in Hebei, China. He received the Ph.D. degree from Beijing Institute of Technology. He is currently with the CETC Network Communication Research Institute.

XUWANG ZHANG is currently with the CETC Network Communication Research Institute.

YOUYONG LIU is currently with the CETC Network Communication Research Institute.